Electron heating in radio-frequency capacitively coupled atmospheric-pressure plasmas

D. W. Liu, F. Iza,[a] and M. G. Kong
Department of Electronic and Electrical Engineering, Loughborough University, Leicestershire LE11 3TU, United Kingdom

(Received 9 September 2008; accepted 8 December 2008; published online 31 December 2008)

In atmospheric-pressure plasmas the main electron heating mechanism is Ohmic heating, which has distinct spatial and temporal evolutions in the α and γ modes. In γ discharges, ionizing avalanches in the sheaths are initiated not only by secondary electrons but also by metastable pooling reactions. In α discharges, heating takes place at the sheath edges and in contrast with low-pressure plasmas, close to 50% of the power absorbed by the electrons is absorbed at the edge of the retreating sheaths. This heating is due to a field enhancement caused by the large collisionality in atmospheric-pressure discharges. © *2008 American Institute of Physics*. [DOI: 10.1063/1.3058686]

Radio-frequency (rf) capacitively coupled plasma (CCP) sources have been the workhorse of the semiconductor industry for several decades.[1] Although for certain applications CCPs have been substituted by other plasma sources, CCPs continue to be an important technological tool in many etching processes. Despite their simple geometrical configuration, CCPs involve complex and interesting physics particularly with regard to the electron heating mechanisms and the resulting electron energy distribution function. Not only are the electrons far from thermodynamic equilibrium but also their energy distribution function presents abrupt transitions when external parameters are varied, e.g., transitions induced by changes in the operating pressure[2] and input power[3] have been reported and are relatively well understood. Most studies, however, have focused on low-pressure discharges for conventional material processing.

In recent years there has been a growing interest on low-temperature plasma sources operating at atmospheric pressure. These sources eliminate the need for costly vacuum systems[4–6] and have potential application in scientific/industrial fields where vacuum operation is not practical, e.g., biomedicine.[7,8] In contrast to low-pressure discharges where nonlocal electron kinetics,[1,9] collisionless heating,[1,2,10] and bounced resonant motion[11] can play important roles, atmospheric-pressure discharges tend to operate in the local regime and are dominated by collisional (Ohmic) heating. This is so because $\nu L/v_{\mathrm{th}} \gg 1$ and $\lambda_\varepsilon \ll L$ are typically satisfied.[1] Here νL is the product of electron collision frequency and gap size, v_{th} is the electron thermal velocity, and λ_ε the electron energy relaxation length. While this is true for most atmospheric-pressure rf discharges with gaps of the order of millimeters, in rf microplasmas where L is reduced to tens of microns nonlocal kinetics of low energy electrons has been reported.[12]

Despite operating in different parameter domains, some of the transitions observed in low-pressure discharges are also present in atmospheric-pressure rf plasmas. In particular, the α-γ transition induced by increasing the input power has been widely studied in atmospheric-pressure discharges.[13–15]

Nevertheless, electron heating in atmospheric-pressure discharges has not been studied as thoroughly as in low-pressure plasmas. This is in part because of the more recent interest on low-temperature atmospheric-pressure discharges and also because of the experimental and theoretical challenges. In this letter, we present experimental and computational results aimed at elucidating the electron heating mechanism in atmospheric-pressure rf discharges. Differences with low-pressure plasmas are highlighted both in the α and the γ modes.

The experimental setup used consists of two water-cooled parallel stainless steel electrodes, each being 2 cm in diameter. The discharge gap is fixed at 2 mm and the system is housed in a Perspex box. Helium flows into the box at 5 SLM (SLM denotes standard liters per minute). A function generator (Tektronix AFG 3102), a rf power amplifier (Amplifier Research 500A100A), and a house-built matching network are used to deliver power to the discharge at 13.56 MHz. The current and the voltage across the discharge are measured with a wideband current probe (Pearson Current Monitor 2877), a wide band voltage probe (Tektronix P5100), and a digital oscilloscope (Tektronix TDS 5054B). An intensified charge-coupled device (iCCD) camera (Andor i-Star DH720) is used to take the images presented in this letter.

To gain a better understanding of the physics governing the discharge, the plasma is simulated using a conventional one-dimensional (1D) model. The model is an extension of the one used in Ref. 16, incorporating the boundary conditions described in Ref. 17. It solves the continuity equation for five species: electrons, He^*, He^+, He_2^* and He_2^+. Due to the large collisionality of the plasma ($\nu \gg \omega_{\mathrm{rf}}$), the inertia of the particles is neglected and the momentum equation is substituted by the drift-diffusion approximation. Furthermore, the energy equation for the electrons is solved assuming a Maxwellian electron energy distribution. Although this assumption is not strictly correct,[12] it has been used in many studies of atmospheric-pressure discharges,[16–19] reaching good agreement with selected experimental data. Finally, the continuity and the energy equations are solved self-consistently with Poisson's equation.

Figure 1 shows the time- and space-resolved optical emission of a rf He discharge in the α mode, in the α-γ

[a]Author to whom correspondence should be addressed. Electronic mail: f.iza@lboro.ac.uk.

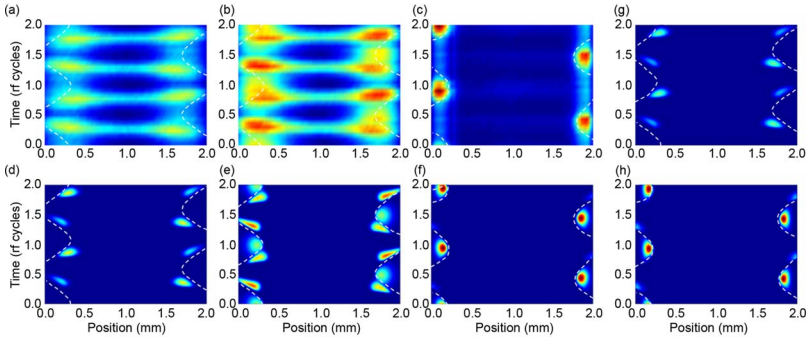

FIG. 1. (Color online) [(a)–(c)] Space- and time-resolved optical emission profiles of an atmospheric-pressure rf He discharge in (a) the α mode (I=31 mA), (b) the α-γ transition (I=93 mA), and (c) the γ mode, I=65 mA. [(d)–(f)] Space- and time-resolved excitation profiles obtained with a 1D fluid code. [(g) and (h)] Space- and time-resolved excitation profiles obtained with a 1D fluid code with the secondary electron coefficient set to 0: (g) low current α mode and (h) high current γ-like mode. White dotted lines indicate the approximate location of the sheath edges.

transition, and in the γ mode. The data shown were obtained by taking a series of 5 ns single shot images at various rf phases, integrating the emission profiles in the radial direction, and collating the results to reconstruct the time evolution. The emission profile is strongly time modulated due to the rapid energy relaxation of energetic electrons at atmospheric pressure (τ_ε=1–10 ps$\ll\tau_{\mathrm{rf}}$=10–100 ns) and the collisional quenching of radiative states. Although the simulations do not model the radiation pattern explicitly, a good agreement is found between the experimentally observed optical emission profiles [Figs. 1(a)–1(c)] and the He excitation profiles predicted in the simulations [Figs. 1(d)–1(f)]. The weak emission observed experimentally in the center of the discharge that is underestimated in the simulation results is attributed to impurities (mostly N_2) present in the experiments and not in the simulation. As seen in Figs. 2(a)–2(c), where the electron power density in the α and γ modes are compared, the simulation results indicate that energy is deposited in the center of the discharge with the same pattern as that of the optical emission shown in Figs. 1(a)–1(c). It is argued that the deposited power leads to the optical emission observed in the experiments, although in the pure He environment of the simulations, electrons do not reach high enough energy as to excite He atoms [Figs. 1(d)–1(f)]. In addition, it is possible that light collected experimentally from out of focus planes contributes to the light recorded in the center of the discharge.

The optical emission of the discharges in the α and γ modes are markedly distinct, with differences in both their spatial and temporal evolutions (Fig. 1). As in low-pressure discharges, the γ mode is characterized by ionization/excitation being mostly sustained by electron avalanches that are created in the high electric fields of the sheaths. In atmospheric-pressure discharges, however, avalanches are not only initiated by secondary electrons but also by electrons generated in pooling reactions among helium metastable atoms and metastable dimers ($He^*+He^*\Rightarrow He^+ +He+e$, $He_2^*+He_2^*\Rightarrow He_2^+ +2He+e$).[20,21] Some of the electrons generated by these reactions are born inside the sheaths seeding avalanches that are similar to those originated by secondary electrons. As a result, it is possible, at least computationally, to obtain a γ-like discharge at atmospheric pressure even in the absence of true secondary electron emissions [as shown in Figs. 1(g) and 1(h)].

In contrast to the γ mode, the α mode is characterized by the power being absorbed mostly at the sheath edges instead of within the sheaths (Fig. 2). As the input power increases and the discharge transitions from the α to the γ mode, the amount of power coupled to the electrons decreases [Fig. 2(d)] and the spatiotemporal evolution of the power density profile changes [Figs. 2(a)–2(c)]. This is true in both low-pressure[1] and atmospheric-pressure discharges. At atmospheric pressure, however, the simultaneous emission in the α mode from the two sheath edges[22] [Fig. 1(a)] that is also captured in the simulation results [Fig. 1(d)] suggests that the electron heating takes place not only during the expansion of the sheath but also during its retreat. In fact, Fig. 2(a) indicates that at atmospheric pressure close to 50% of the input power delivered to the electrons is absorbed in the neighborhood of the retreating sheaths. This contrasts with the situation encountered in low-pressure He discharges, where the heating is appreciable only during the expansion of the sheath.[1] Simulation results show that the heating in the neighborhood of the retreating sheath decreases rapidly with decreasing pressure and as a result, while at atmospheric pressure He excitation takes place simultaneously at both sheath edges (expanding and retreating), at 2 Torr the excitation is completely dominated by the expanding sheath [cf. Figs. 3(a) and 3(b)].

The additional heating of the electrons in atmospheric-pressure discharges is caused by the formation of a field-enhanced region at the retreating sheath edge [Fig. 3(c)]. While at low pressure electrons can diffuse fast enough to follow the retreating sheath, at atmospheric pressure collisions prevent electrons from diffusing fast enough. As a result, electrons are not able to follow the retreating sheath merely by diffusion, and a self-consistent electric field builds up to drive the electrons. The electric field develops when electrons not being able to diffuse fast enough toward the retreating sheath pile up at the edge, creating a region of negative space charge [Fig. 3(d)]. The resulting electric field accelerates the electrons toward the electrode, helping them to follow the retreating sheath and heating them in the process.

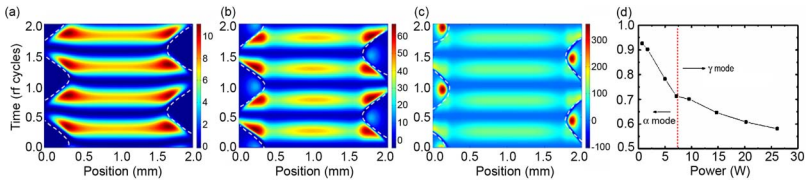

FIG. 2. (Color online) Power absorbed by the electrons calculated as J_eE (mW/cm^3) from the simulation data. Here. J_e is the electron current density and E is the electric field. (a) α mode. (b) α-γ transition. (c) γ mode. (d) Percent of input power dissipated by the electrons calculated as $J_eE/J_{\mathrm{tot}}E$.

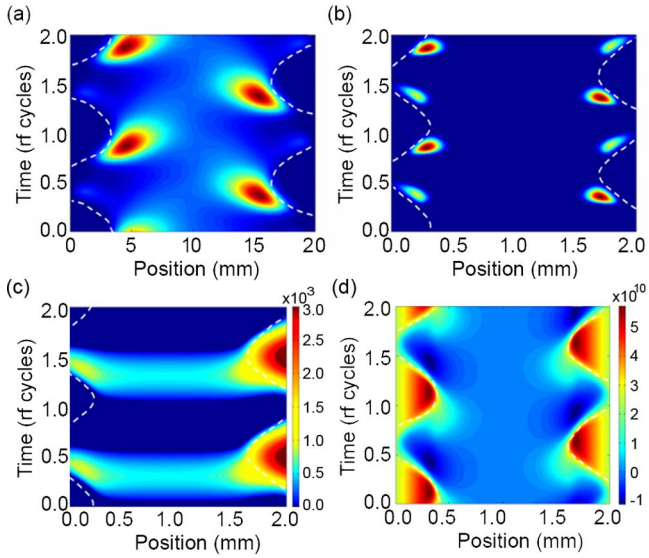

FIG. 3. (Color online) Simulation results. [(a) and (b)] Space- and time-resolved helium excitation profiles in a rf He discharge at (a) 2 Torr and (b) 760 Torr. (c) Electric field and (d) space charge in an atmospheric-pressure rf He discharge. In (c), negative values are set to 0 to facilitate the visualization of the evolution of the field profile.

Although heating at the edge of retreating sheaths is negligible in low-pressure discharges of noble gases (in fact collisionless interaction of electrons with retreating sheaths leads to cooling of the electrons),[1] a similar heating mechanism has been observed in low-pressure rf discharges when the electrons are subject to an increased collisionality in the presence of molecular gases.[23] It is noted, however, that while at low pressure heating at the retreating sheath edge is accompanied by a strong field reversal,[23] at atmospheric pressure no field reversal is observed [Fig. 3(c)]. Instead, a region of enhanced electric field without changes in field polarity is formed at the retreating sheath edge.

In conclusion, atmospheric-pressure glow discharges are sustained by Ohmic heating of the electrons. In the α mode, the electrons are heated both during the expansion and the retreat of the sheaths. This is observed both in time-resolved experimental and computational measurements and results in a simultaneous emission from both sheath edges. In the γ mode, the heating takes place mostly in avalanches across the sheaths, giving rise to an emission pattern that alternates between the two electrodes. While secondary electrons seem to be the primary source of seed electrons for the avalanches in the γ mode, a contribution from metastable pooling reactions is also identified as a source of seed electrons in atmospheric-pressure discharges.

This work was funded by the Engineering and Physical Sciences Research Council, U.K. The authors are grateful to Dr. T. Mussenbrock (Ruhr University Bochum) for valuable discussions related to this work.

[1] M. A. Lieberman and A. J. Lichtenberg, *Principles of Plasma Discharges* (Wiley, New Jersey, 2005).
[2] V. A. Godyak and R. B. Piejak, Phys. Rev. Lett. **65**, 996 (1990).
[3] V. A. Godyak, R. B. Piejak, and B. M. Alexandrovich, Phys. Rev. Lett. **68**, 40 (1992).
[4] A. Ladwig, S. Babayan, M. Smith, M. Hester, W. Highland, R. Koch, and R. Hicks, Surf. Coat. Technol. **201**, 6460 (2007).
[5] A. Sharma, A. Pruden, O. Stan, and G. J. Collins, IEEE Trans. Plasma Sci. **34**, 1290 (2006).
[6] C. Sarra-Bournet, S. Turgeon, D. Mantovani, and G. Laroche, Plasma Processes Polym. **3**, 506 (2006).
[7] F. Iza, G. J. Kim, S. M. Lee, J. K. Lee, J. L. Walsh, Y. T. Zhang, and M. G. Kong, Plasma Processes Polym. **5**, 322 (2008).
[8] G. Fridman, G. Friedman, A. Gutsol, A. B. Shekhter, V. N. Vasilets, and A. Fridman, Plasma Processes Polym. **5**, 503 (2008).
[9] V. I. Kolobov and V. A. Godyak, IEEE Trans. Plasma Sci. **23**, 503 (1995).
[10] M. M. Turner, Phys. Rev. Lett. **75**, 1312 (1995).
[11] G. Y. Park, S. J. You, F. Iza, and J. K. Lee, Phys. Rev. Lett. **98**, 085003 (2007).
[12] F. Iza, J. K. Lee, and M. G. Kong, Phys. Rev. Lett. **99**, 075004 (2007).
[13] J. J. Shi and M. G. Kong, IEEE Trans. Plasma Sci. **33**, 624 (2005).
[14] S. Y. Moon, J. K. Rhee, D. B. Kim, and W. Choe, Phys. Plasmas **13**, 033502 (2006).
[15] X. Yang, M. Moravej, G. R. Nowling, S. E. Babayan, J. Penelon, J. P. Chang, and R. F. Hicks, Plasma Sources Sci. Technol. **14**, 314 (2005).
[16] J. J. Shi and M. G. Kong, Phys. Rev. Lett. **96**, 105009 (2006).
[17] Q. Wang, D. J. Economou, and V. M. Donnelly, J. Appl. Phys. **100**, 023301 (2006).
[18] H. C. Kim, F. Iza, S. S. Yang, M. Radmilovic-Radjenovic, and J. K. Lee, J. Phys. D **38**, R283 (2005).
[19] P. S. Kothnur and L. L. Raja, J. Appl. Phys. **97**, 043305 (2005).
[20] S. Rauf and M. J. Kushner, J. Appl. Phys. **85**, 3460 (1999).
[21] R. Deloche, P. Monchicourt, M. Cheret, and F. Lambert, Phys. Rev. A **13**, 1140 (1976).
[22] D. Liu, F. Iza, and M. G. Kong, IEEE Trans. Plasma Sci. **36**, 952 (2008).
[23] M. M. Turner and M. B. Hopkins, Phys. Rev. Lett. **69**, 3511 (1992).